Reentrant valence transition in $YbCu_{4.5}$ under pressure

Hitoshi Yamaoka,[1,*] Naohito Tsujii,[2] Yoshiya Yamamoto,[3] Yuichi Michiue,[4] Jung-Fu Lin,[5,6] Nozomu Hiraoka,[7] Hirofumi Ishii,[7] Ku-Ding Tsuei,[7] and Jun'ichiro Mizuki[3]

[1]*RIKEN SPring-8 Center, 1-1-1 Kouto, Sayo, Hyogo 679-5148, Japan*

[2]*International Center for Materials Nanoarchitectonics (MANA), National Institute for Materials Science, 1-2-1 Sengen, Tsukuba, Ibaraki 305-0047, Japan*

[3]*Graduate School of Science and Technology, Kwansei Gakuin University, Sanda, Hyogo 669-1337, Japan*

[4]*International Center for Materials Nanoarchitectonics (MANA), National Institute for Materials Science, 1-1 Namiki, Tsukuba, Ibaraki 305-0047, Japan*

[5]*Department of Geological Sciences, The University of Texas at Austin, Austin, Texas 78712, USA*

[6]*Center for High Pressure Science and Technology Advanced Research (HPSTAR), Shanghai 201203, China*

[7]*National Synchrotron Radiation Research Center, Hsinchu 30076, Taiwan*

(Received 23 July 2017; revised manuscript received 14 January 2018; published 2 February 2018)

The electronic structure of $YbCu_{4.5}$ under pressure has been studied with x-ray emission spectroscopy. Pressure-induced first-order valence transition to the divalent Yb state is found around 0.6–2.7 GPa, accompanied by the structural transition at the same pressure range of 0–1.0 GPa suggested by the change in the x-ray diffraction pattern. We also measured temperature dependencies of the Yb valence and magnetic susceptibility, which are compared with the single impurity Anderson model.

DOI: 10.1103/PhysRevB.97.085106

I. INTRODUCTION

In $4f$-electron systems Eu, Sm, Tm, and Yb compounds often show the valence fluctuation phenomena because of the small energy difference between the two charge states [1]. Physical properties of the valence fluctuation systems are well described by the competition between magnetic order caused by the Rudermann-Kittel-Kasuya-Yosida (RKKY) interaction and the Kondo effect with the Doniach phase diagram [2,3]. The magnetic order is caused by localized nature, while the Kondo effect is the screening of the local moment through the Kondo singlet formation. The Kondo interaction has been described theoretically by the single impurity Anderson or periodic Anderson models, where thermodynamic properties can be characterized by the Kondo temperature (T_K) and the c-f hybridization strength. It is noted that hydrostatic pressure can control the Kondo temperature of the system ideally without local distortion, which is possibly caused by chemical substitution. In the Yb compound, the Yb valence often fluctuates between magnetic $4f^{13}$ (Yb^{3+}) and nonmagnetic $4f^{14}$ (Yb^{2+}) states. In the Yb system, T_K decreases with pressure and the Yb^{3+} state is favored at higher pressures because of the smaller ionic radius of Yb^{3+} ions compared to the ionic radius of Yb^{2+} ions.

In the phase diagram of the Yb-Cu binary alloy system, the compositions of YbCu, $YbCu_2$, $YbCu_{3.5}$, $YbCu_{4.25}$, $YbCu_{4.4}$, $YbCu_{4.5}$, and $YbCu_{6.5}$ appear [4–7]. X-ray absorption spectroscopy at the Yb L_3 edge showed the valence fluctuating Yb valence state; the Yb valence of YbCu, $YbCu_2$, $YbCu_{3.5}$, $YbCu_{4.5}$, and $YbCu_{6.5}$ were 2.37, 2.39, 2.89, 2.96, and 2.40, respectively [8]. A compound with $YbCu_5$ stoichiometry had been thought not to exist [5]. However, it was synthesized with a high-pressure technique later [9]. YbCu and $YbCu_2$ have orthorhombic crystal structures of FeB-type and CeCu-type, respectively [4]. The crystal structures of the Cu-rich phases were very complicated. The crystal structure of $YbCu_{3.5}$ has not been clarified yet [4]. $YbCu_{4.4}$ and $YbCu_{4.25}$ were based on $AuBe_5/MgCu_2$-type substructures with approximately 4570 and 2780 atoms per unit cell, respectively [7]. $YbCu_{6.5}$ is related to the $CaCu_5$ structure including the 18% Ca site occupied by pairs of Cu atoms [5]. Among them, $YbCu_{4.5}$ may be the most interesting compound because of the specific heat coefficient of $\gamma \sim 635$ mJ/mol K^2 mol, which is so far the heaviest fermion state among the Yb-based systems with a nonmagnetic ground state [5,10,11]. The heavy-fermion state was enhanced under pressure to 740 mJ/mol K^2 at 0.82 GPa [8,12]. In $YbCu_{4.5}$, no magnetic order was observed up to 23.5 GPa and down to 50 mK [13].

In this paper we report the pressure-induced change in the electronic state and crystal structure of $YbCu_{4.5}$. We employ partial fluorescence yield x-ray absorption spectroscopy (PFY-XAS) to study the valence of the Yb ions [14,15]. In $YbCu_{4.5}$, the electronic structure under pressure has not been explored so far. We find a first-order reentrant valence transition to the lower valence state induced by pressure, where the structural transition also occurs. Magnetic susceptibility measurements and x-ray diffraction (XRD) are performed. We also measure the temperature dependence of the Yb valence. The results of the magnetic susceptibility and the temperature-induced change in the Yb valence are compared to the single Anderson impurity model. The theoretical fits are not satisfactory. This suggests that the Yb valences are site dependent due to the complex crystal structure.

*yamaoka@spring8.or.jp

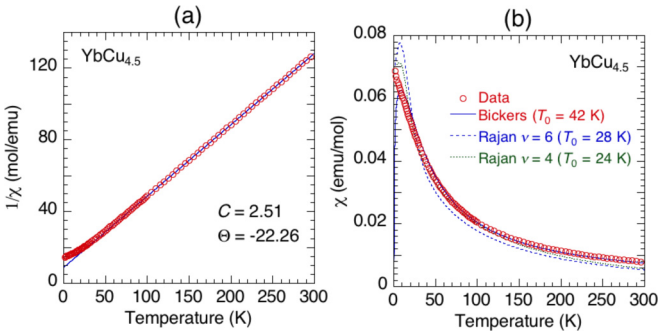

FIG. 1. (a) Temperature dependence of the inverse of the magnetic susceptibility (open circles) of $YbCu_{4.5}$. Solid line is a fit with the Curie-Weiss law for the data at $T > 100$ K. (b) Temperature dependence of the magnetic susceptibility (open circles) with the fits based on the single impurity Anderson model by Bickers *et al.* (solid line) and Rajan (dashed and dotted lines).

II. EXPERIMENTS

Ytterbium (3N) and copper (5N) were melted at a molar ratio of 1 : 4.5 by resistive heating in a tantalum tube. The chemical composition $YbCu_{4.5}$ was determined by electron probe microanalysis. The magnetic susceptibility was measured with a SQUID (superconducting quantum interference device) magnetometer (Quantum design, MPMS5S) at an applied field of 1000 Oe.

Pressure dependence of the x-ray powder diffraction patterns were measured at BL12B2, SPring-8, using a 3-pin plate diamond anvil cell (DAC, Almax easyLab Industries) with a CCD detection system at room temperature. We take an arrangement of both incoming and outgoing x-ray beams passing through the diamonds with an incident photon energy of $h\nu = 18$ keV. A two-dimensional image of the CCD system was integrated by using the FIT2D program [16].

PFY-XAS measurements were performed at the Taiwan beamline BL12XU, SPring-8. Details of the experimental setup have been published elsewhere [14,15,17]. The overall energy resolution was estimated to be about 1 eV around the emitted photon energy of 7400 eV from the elastic scattering. The high-pressure conditions were reached using a diamond anvil cell (DAC) with a Be gasket and the pressure-transmitting medium was silicone oil. A membrane-controlled DAC was used for a high-pressure experiment at room temperature. The pressure was measured based on the Raman shift of the ruby fluorescence [18,19].

III. RESULTS AND DISCUSSION

A. Magnetic susceptibility

The temperature dependence of the inverse magnetic susceptibility $1/\chi$ of $YbCu_{4.5}$ is shown in Fig. 1(a). The inverse susceptibility should be a linear function of T as $1/\chi = (T - \Theta_p)/C$, $C = (N_A\mu_{\rm eff}^2)/(3k_B)$, at temperatures high enough where both Kondo and crystalline field effect (CEF) effects are less important, where C, Θ_p, N_A, $\mu_{\rm eff}$, and k_B are Curie constant, Weiss temperature, Avogadro number, effective magnetic moment, and Boltzmann constant, respectively. We estimated the Curie constant, the Weiss temperature, and the effective magnetic moment from the slope of the linear part of $1/\chi$ ($100 < T < 300$ K) to be 2.51 emu/mol K, -22.3 K, and 4.48 μ_B, respectively. The effective magnetic moment is consistent with the values of 4.36 ± 0.04 μ_B measured by Spendeler *et al.* [8]. The effective magnetic moment of Yb^{3+} ion is 4.53 μ_B and the Yb valence of $YbCu_{4.5}$ is nearly Yb^{3+}. However, negative Weiss temperatures suggest that Yb of $YbCu_{4.5}$ is slightly valence fluctuating.

According to the Bethe-Ansatz solution of the Coqblin-Schrieffer model, the physical properties of a Kondo system are well scaled by a single energy parameter (T_0). The characteristic temperature is related to the magnetic susceptibility $\chi(0)$ at 0 K by $\chi(0)T_0 = [N_A\nu(\nu-1){g_L}^2\mu_B^2]/(24\pi k_B)$, where ν is the ground state degeneracy, g_L is the Landé factor, and μ_B is the Bohr magnetron [20,21]. We derived the characteristic temperature (T_0) from $\chi(0)$ to be $T_0 = 47$ K and $T_K = 25$ K assuming the relation $T_0 = (2J+1)T_L/2\pi$ and $T_K = 0.6475T_L$ for $J = 7/2$ [22]. This value is comparable to $T_K = 15$ K, which was derived from the maximum of the resistivity data and the minimum of the thermoelectric power of the temperature dependence [8,12].

The characteristic temperatures could be estimated by using the Rajan's numerical result based on the Coqblin-Schrieffer model [21]. We fit the Rajan's curve to the experimental result of the magnetic susceptibility, making T_0 a fit parameter as shown in Fig. 1(b). T_0 is estimated to be 28 K for $\nu = 6$ and 24 K for $\nu = 4$. The theory, however, does not reproduce the temperature dependence of the magnetic susceptibility well. Rajan also showed a relation of T_0 with γ as $\gamma_{\rm CS} = [N_A(\nu-1)\pi k_B]/(6T_0)$ [21]. T_0 is estimated to be 48 K with this formula assuming $\gamma = 635$ mJ/K^2 mol.

We also apply a theoretical universal curve based on the single impurity Anderson model (SIAM) by Bickers *et al.* [23]. T_0 is estimated to be 42 K, which is in the same order as the values derived above. The theoretical fits to the experimental data are not fully satisfactory, indicating that the temperature dependence of the magnetic susceptibility cannot be fully understood within the SIAM.

T^2 dependence of the resistivity was observed only at temperatures below 400 mK at 23.5 GPa [24]. The Kondo temperature decreases with pressure in Yb compounds and thus the coherent temperature may be much higher than 400 mK at ambient pressure. Normally the coherent temperature to form the Kondo lattice, where the T^2 dependence of the resistivity is observed, is one order less than the Kondo temperature [9,25]. The characteristic temperature T_0 is proportional to the Kondo temperature T_K as described above. Therefore, the above estimated values of T_0 seems to be reasonable when we consider the coherent temperature.

B. X-ray diffraction

Physical properties of $YbCu_{4.5}$ are similar to the physical properties of cubic $YbCu_5$, but the crystal structure is very complicated. The crystal structure of $YbCu_{4.5}$ was solved using x-ray diffraction and high-resolution transmission electron microscopy by Černý *et al.* [26]: a monoclinically distorted $7 \times 7 \times 6.5$ superstructure of the cubic $AuBe_5$ structure type with 7448 atoms per unit cell. This is one of the most complex systems found among intermetallic compounds. Such a

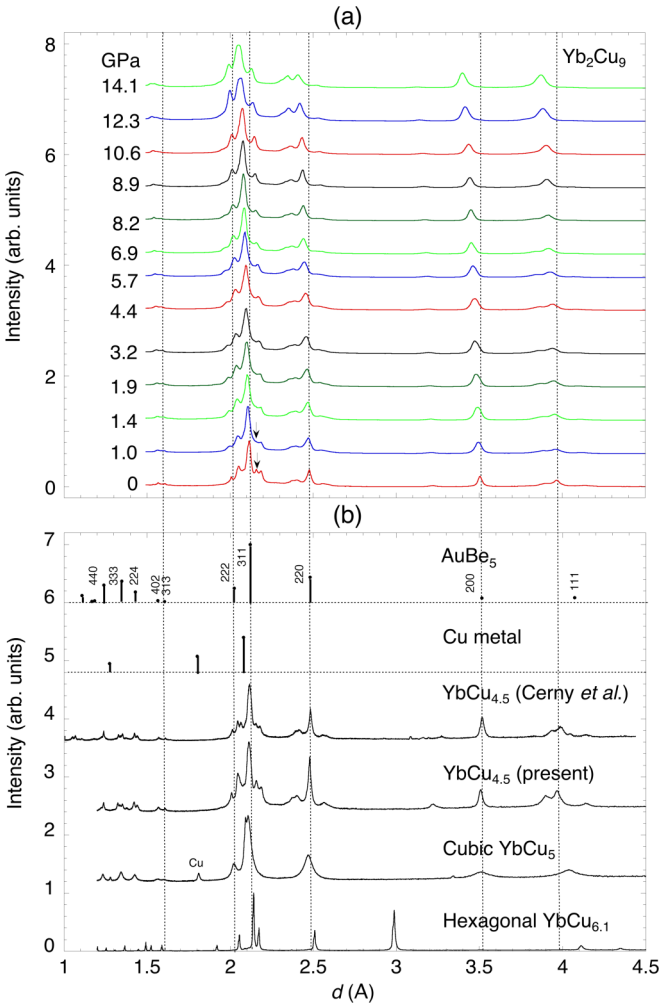

FIG. 2. Comparison of the XRD patterns of (a) $YbCu_{4.5}$ (present results as a function of pressure) and (b) $YbCu_{4.5}$ measured by Černý *et al.*, cubic $YbCu_5$, and hexagonal $YbCu_{6.1}$ at room temperature [9,26,27]. The data in (a) and (b) were measured at 18 keV ($\lambda = 0.68467$ Å) and by the Cu $K\alpha$ line ($\lambda = 1.5406$ Å), respectively. Arrow in (a) is marked on a peak which disappears above 1.0 GPa. The horizontal axis is converted to the lattice distance (d) from the diffraction angle using the Bragg relation for comparison. The hexagonal phase of $YbCu_{6.1}$ is nominal composition. The intensity in (a) is normalized by the peak intensity. In (b) the calculated peaks for an $AuBe_5$-type crystal structure and Cu metal are also shown.

complicated crystal structure makes band-structure calculations difficult. Iandelli and Palenzona suggested the crystal structure based on a tetragonal cell derived from the $AuBe_5$ type, although they could not identify the exact structure [4]. The crystallographic properties with a superstructure of $YbCu_{4.5}$ was also studied by Spendeler *et al.* [8]. The crystal structure of $YbCu_{4.5}$ was solved in 1996 by Černý *et al.* [26].

Figure 2(a) shows a comparison of the XRD patterns of $YbCu_{4.5}$ (present results as a function of pressure), $YbCu_{4.5}$ measured by Černý *et al.*, cubic $YbCu_5$, and hexagonal $YbCu_{6.1}$ at room temperature [9,26,27]. In the pressure dependence of the XRD patterns of $YbCu_{4.5}$, a peak at $2\theta \sim 18.2°$ disappeared above 1.0 GPa as shown in Fig. 2(a) by arrows. The other peaks do not change the intensity significantly.

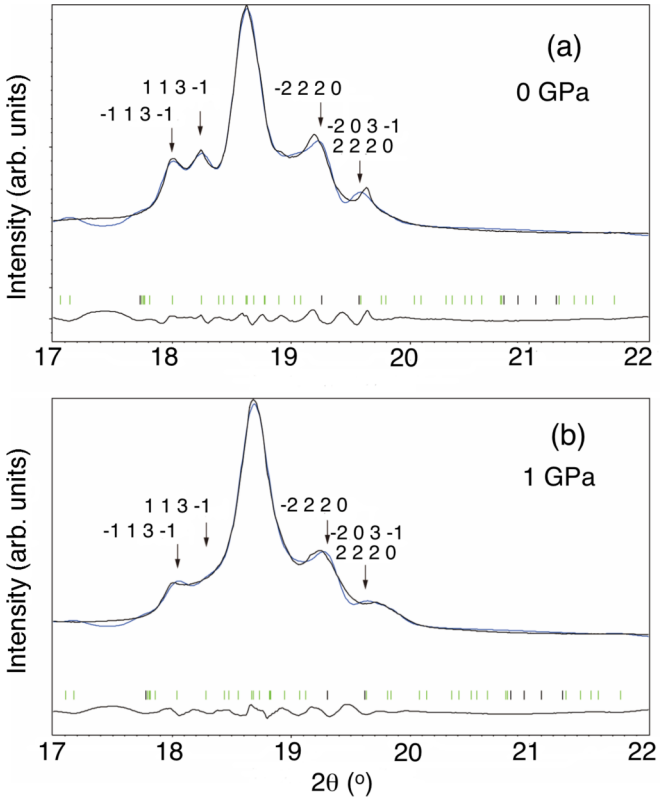

FIG. 3. XRD patterns of $YbCu_{4.5}$ at $2\theta = 17°$–$22°$ measured at (a) 0 GPa and (b) 1 GPa with the peak indices assigned by the Le Bail method.

This suggests a structural transition at the pressure between 0 and 1.0 GPa, which corresponds to the pressure where the valance transition occurred as described below. In $YbCu_{4.5}$ in Fig. 2(a) the peaks around $d = 3.5$ Å ($2\theta = 10.1°$), 2.49 Å ($2\theta = 14.4°$), and 2.11 Å ($2\theta = 16.9°$) correspond to (200), (220), and (311) reflections of the original AuBe-type subcell, respectively. This indicates that $YbCu_{4.5}$ is derived from the cubic AuB_5-type crystal domains [26].

Figure 2(b) includes the XRD pattern of the present $YbCu_{4.5}$ sample measured using a laboratory source, which matched well with the reproduced XRD pattern measured by Černý *et al.* [26], indicating a reliability of the sample quality. In the high-pressure experiments we used the same samples.

It is difficult to make Rietveld refinements only with the XRD data. Instead, the XRD patterns at $P = 0$ and 1 GPa were analyzed by the Le Bail method using the JANA2006 software [28]. The analysis was performed with the four-dimensional superspace based on the structure model suggested by Černý, where the $AuBe_5$-type monoclinic subcell is modulated along the c direction to form a $7 \times 7 \times 13$ supercell [26]. Figures 3 and 4 show the XRD patterns measured at the pressure of 0 and 1 GPa with the peak indices obtained by the Le Bail analysis. The lattice constants of the monoclinic subcell at $P = 0$ GPa were given to be $a = 7.0042(11)$ Å, $b = 7.0198(12)$ Å, $c = 7.0640(11)$ Å, $\beta = 91.381(6)°$, while those for $= 1$ GPa were obtained to be $a = 6.9867(13)$ Å, $b = 7.0041(18)$ Å, $c = 7.0509(15)$ Å, $\beta = 91.363(6)°$. It is found that the peak indexed by (113-1) shows a sudden drop in

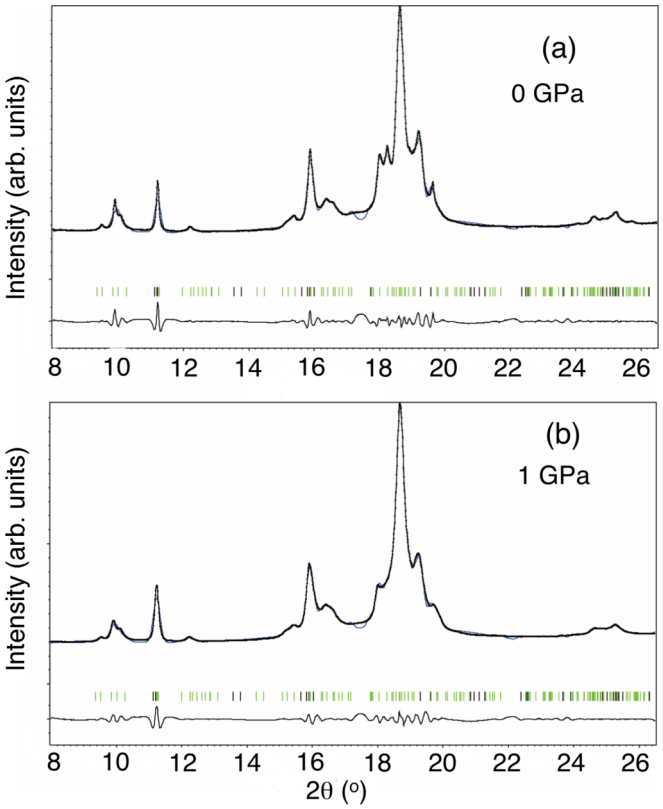

FIG. 4. XRD pattern of $YbCu_{4.5}$ at $2\theta = 8°$–$26.5°$ measured at (a) 0 GPa and (b) 1 GPa with the fitting results by the Le Bail method.

its intensity between 0 and 1 GPa. This change occurs suddenly at this pressure range, pointing to the existence of a structural phase transition.

The change in the d spacings for the peaks corresponding to the (200), (220), and (311) reflections of the original $AuBe_5$-type subcell are shown in Fig. 5. The lattice shrinks smoothly up to 8.9 GPa, while the trend changes above 10.6 GPa. The disappearance of the (113-1) peak for the supercell above 1.0 GPa seems not to change the lattice parameters significantly.

At present, the details of this structure change is unclear. Since there is no clear anomaly in the pressure dependence

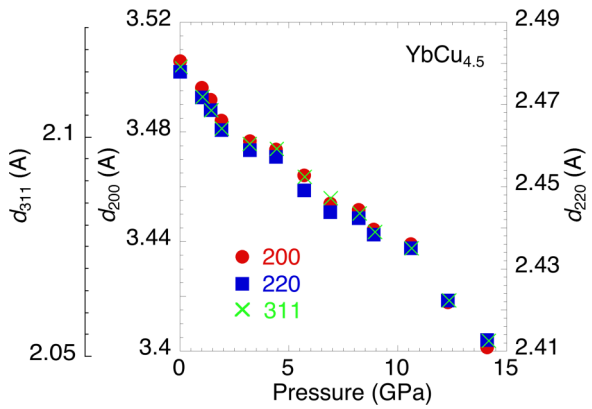

FIG. 5. Pressure dependence of d (Å) of the peaks corresponding to the (200), (220), and (311) reflections of the original $AuBe_5$-type subcell.

of the d spacings for the peaks corresponding to the (200), (220), and (311) reflections of the original $AuBe_5$-type subcell. Hence, the lattice volume is not likely to change drastically at the phase transition pressure P_c. Instead, it is more likely that the local coordination environment of Cu atoms around Yb may change at P_c, which should be addressed in the future. Note that comparison with the XRD patterns of cubic $YbCu_5$ and hexagonal $YbCu_5$ indicates no structural transition to the hexagonal crystal structure above 1.0 GPa.

C. X-ray absorption spectroscopy

Pressure dependence of the PFY-XAS spectra is shown in Fig. 6(a). In Fig. 6(b) we show an example of the fit at 21.2 GPa assuming a quadrupole component at 8934 eV, one component for Yb^{2+}, and two components for Yb^{3+}. The Yb valence of $YbCu_{4.5}$ is approximately 2.96 at ambient pressure, which is nearly the same as that of cubic $YbCu_5$ [29]. A striking pressure-induced change in the Yb valence is observed at the low pressure range less than 2.7 GPa as shown in Fig. 6(c), indicating a first-order valence transition. Recently we found a pressure-induced reentrance to the Yb^{2+} state in cubic $YbAg_xCu_{5-x}$ without any structural transition [30]. On the other hand, in $YbCu_{4.5}$, this pressure range of the first-order valence transition corresponds to the occurrence of the structural phase transition pressure mentioned above. The Yb valence seems to continue decreasing slightly up to 6.3 GPa after the first-order valence transition and starts to increase gradually above 9.2 GPa, suggesting that two phases may coexist in the pressure range between 2.67 and 6.3 GPa. Such a pressure-induced reentrant valence transition with the structural transition has been observed in EuO [31,32].

In $YbCu_{4.5}$, anomalous behavior has been observed in the temperature dependence of the resistivity under pressure [8,13,24]. The resistivity took a maximum ($T_\rho^{\max}$) with decreasing temperature, which has been considered to correlate to the Kondo temperature (T_K). Pressure dependence of $T_\rho^{\max}$ showed a minimum at ~10 GPa [8,13,24]. The increase of $T_\rho^{\max}$ above 10 GPa does not connect to T_K at high pressures because the Yb valence increases above 10 GPa as shown in Fig. 6(c), indicating the decrease of T_K with pressure. This behavior can be attributed to the CEF effect, where T_K is smaller than T_{CEF} and a Kondo scattering with the state populated thermally to the higher CEF level occurred [24]. It is interesting that the resistivity data normalized to the maximum of the resistivity separated to be two groups: one below 3.1 GPa and one above 10 GPa [24]. This could be explained from the pressure-induced change in the Yb valence and the characteristic behavior of the resistivity at <3.1 GPa, which may originate from the valence transition.

Figure 7(a) shows the temperature dependence of the PFY-XAS spectra. A slight increase of the Yb^{2+} intensity and decrease of the Yb^{3+} intensity is observed. The mean Yb valence estimated is shown in Fig. 7(b) as a function of temperature. In Fig. 7(b) a χT curve is also plotted. The χT curve shows a similar trend as the change in the Yb valence. Such correlation between temperature dependence of the χT and the Yb valence has also been observed in the $YbInCu_4$-based compounds [33].

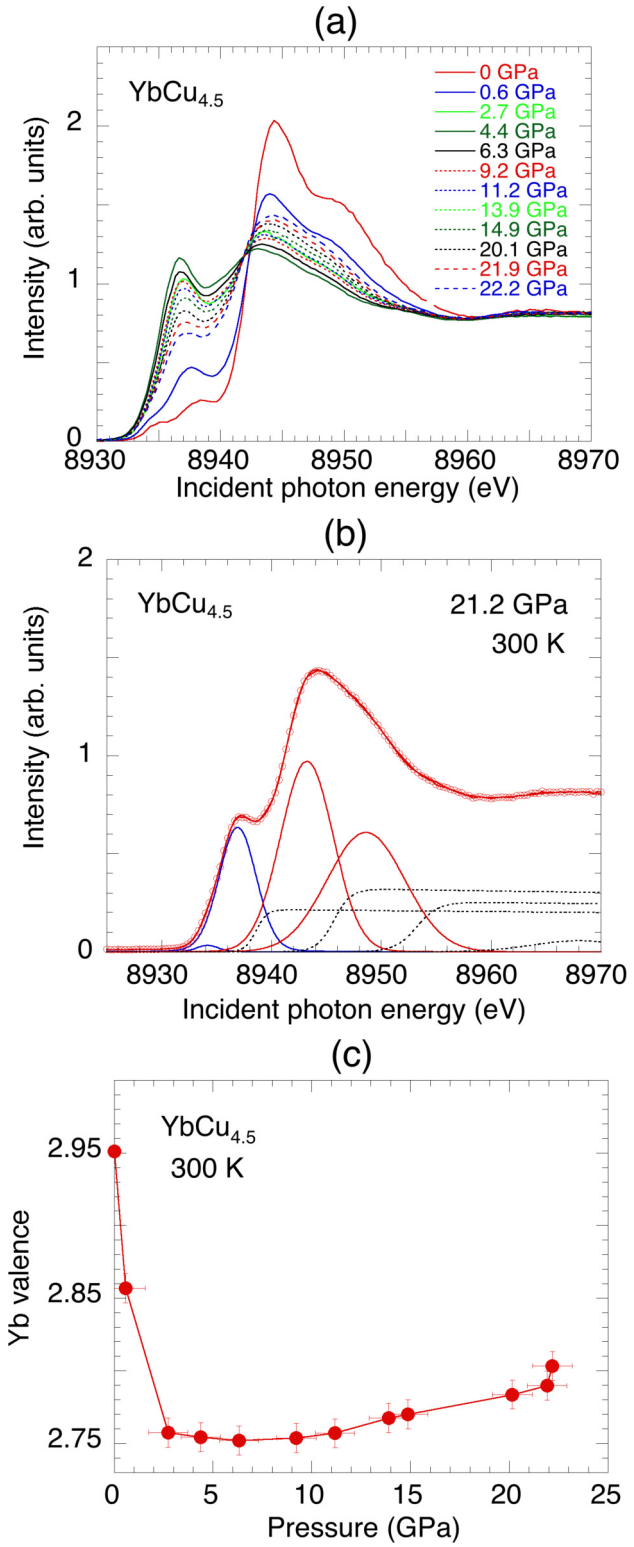

FIG. 6. (a) Pressure dependence of the PFY-XAS spectra of $YbCu_{4.5}$ at 300 K. (b) A fit example of the PFY-XAS spectrum at 21.2 GPa. (c) Pressure dependence of the Yb valence estimated from the fits to the PFY-XAS spectra.

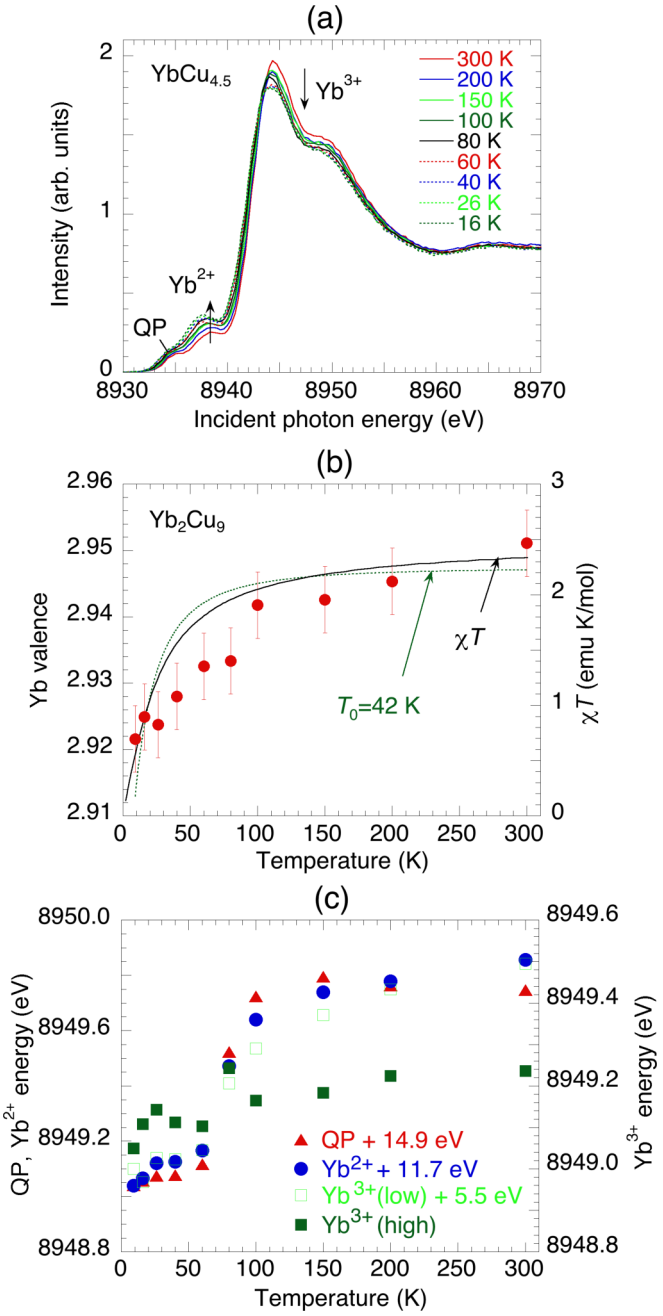

FIG. 7. The experimental results of XES are shown. (a) Temperature dependence of the PFY-XAS spectra at ambient pressure. Arrows in (a) correspond to the direction to decrease the temperature. (b) Temperature dependence of the Yb valence (closed circles, left vertical axis) estimated from the fits to the PFY-XAS spectra and χT (solid line, right vertical axis). The dotted line is an Anderson model fit assuming the characteristic temperature of 42 K. (c) Temperature dependence of the peak energy positions of Yb^{3+} [major peak (low energy) and minor (high energy)], Yb^{2+}, and quadrupole (QP) components. Energy positions of each component are shifted for comparison.

In the single impurity Anderson model, the temperature dependence of the valence $v(T)$ follows the equation $v(T) = 2 + n_f(\infty) - [\Delta n_f(T)/\Delta n_f(0)]\Delta n_f(0)$, where $n_f(\infty)$ and $\Delta n_f(T)$ are the intermediate temperature limit of the valence and the total decrease in valence, respectively [14,23]. $\Delta n_f(T)/\Delta n_f(0)$ was calculated as a function of T/T_0. We use $T_0 = 42$ K, which was obtained from the fit to the susceptibility. $n_f(\infty)$ is estimated using the following

relations. Calculations using the large degeneracy expansion method suggested that the characteristic temperature related to the Kondo effect T_0 can be expressed as [23] $T_0 = Dg^{1/6}e^{-1/6g}(D/\Delta)^{8/6}$, where D, Δ, and g are the width of the conduction band, the energy of the spin-orbit coupling, and $g = 1 - n_f(\infty)$, respectively. We can deduce the D according to the relations: $D = (\ln 2)^{1/2}W = 2.190n_e/\gamma(0)$, where $N(\varepsilon_f)$, n_e, W, and $\gamma(0)$ are DOS at Fermi level, number of valence electrons, Gaussian DOS width, and electronic specific coefficient in units of mJ/mol K^2 for the case without hybridization, respectively. [29] We estimate D value for the experimental value of $\gamma(0)$ and then obtain $n_f(\infty)$. However, here $\gamma(0)$ is not available in $YbCu_{4.5}$ and we assume $D =$ 0.5 eV [$n_f(\infty) = 0.947$ and $\gamma(0) = 66$ mJ/mol K^2] as a reasonable value [34]. In Fig. 4(b) a theoretical fit based on the single impurity Anderson model is also plotted assuming the characteristic temperature of 42 K derived in the fit to the magnetic susceptibility in Fig. 1(b). The fit curve describes temperature-induced overall behavior of the Yb valence roughly, but it does not reproduce the experimental result well.

In Fig. 7(c) we also show the temperature dependence of the peak energy positions of Yb^{3+} (major peak) and Yb^{2+} components. It is well known that the change in the charge state induces the shift of the absorption edge. The peak energy positions of the quadrupole Yb^{2+} and major Yb^{3+} components in Fig. 4(c) follow the temperature-induced change in the mean Yb valence well and show the change in the trend below 70 K, although the minor Yb^{3+} component is relatively insensitive to the temperature.

It is noted that $YbCu_{4.5}$ has three types of Yb sites crystallographically: in the $AuBe_5$-type regions, near the antiphase boundaries, and near shear planes with the relative abundances of 2 : 1 : 1 [26]. The three Yb sites possibly show a different temperature-induced behavior for the Yb valence state and thus, it may be difficult to describe the result with a single characteristic temperature. It is also noted that the CEF effect was not taken into account in the present analyses [23]. The Yb valence will be changed if CEF is comparable or higher than T_K. Actually, if CEF is strong, it reduces the eightfold degeneracy of $J = 7/2$ in Yb^{3+} at low temperature [9].

D. Conclusion

The XES and XRD studies have been performed under pressure for $YbCu_{4.5}$. The XRD spectra showed a structural phase transition at 0–1.0 GPa. The XES data showed a first-order valence transition at 0.6–2.7 GPa. This is an unusual valence transition since the Yb valence abruptly decreases from $Yb^{2.95+}$ to $Yb^{2.76+}$, which is contrasting to the normal behavior where the valence increases toward Yb^{3+} state with pressure [30]. Both XRD and XES results indicate the first-order valence and structural transitions occur at 0.6–1.0 GPa in $YbCu_{4.5}$. Pressure-induced change in the Yb valence correlates to the resistivity data well. Temperature dependence of the Yb valence was also studied, showing the decrease of the Yb valence at low temperatures. Overall behavior in the temperature dependencies of the magnetic susceptibility and Yb valence could be described with the conventional single impurity Anderson model, but is not satisfactory, and the Kondo temperature seems to be overestimated. This may be partly attributed to the complex crystal structure including the three crystallographic Yb sites.

ACKNOWLEDGMENTS

The experiments were performed at Taiwan beam lines BL12XU and BL12B2 at SPring-8 under Proposals Nos. 2012A4265, 2012B4256, 2015A4129, 2015A4258, 2015B4258, and 2015B4133 (corresponding proposals Nos. 2011-2-021, 2012-3-012, and 2015-2-033 of NSRRC). This work is partly supported by a Grant in Aid for Scientific research from the Japan Society for the Promotion of Science (Kiban C 22540343 and Kiban C 15K05194). We deeply thank Jin-Min Chen, Jenn-Min Lee, and Takuma Kawai for their kind help in the XRD study. J.F.L. acknowledges support from HPSTAR. We also thank Radovan Černý for the use of their XRD pattern of $YbCu_{4.5}$ and useful discussion.

[1] P. Strang, A. Svane, W. M. Temmerman, Z. Szotek, and H. Winter, Understanding the valency of rare earths from first-principles theory, Nature (London) **399**, 756 (1999).

[2] S. Doniach, The Kondo lattice and weak antiferromagnetism, Physica B&C (Amsterdam) **91**, 231 (1977).

[3] J. M. Lawrence, P. S. Riseborough, and R. D. Parks, Valence fluctuation phenomena, Rep. Prog. Phys. **44**, 1 (1981).

[4] A. Iandelli and A. Palenzona, The ytterbium-copper system, J. Less-Common Met. **25**, 333 (1971).

[5] J. Hornstra and K. H. J. Buschow, The crystal strucure of $YbCu_{6.5}$, J. Less-Common Met. **27**, 123 (1972).

[6] M. Giovannini, R. Pasero, S. De Negri, and A. Saccone, Yb(Cu, T)$_5$ and Yb(Cu, T)$_{4.5}$ solid solutions (T = Ag, Au, Pd), Intermetallics **16**, 399 (2008).

[7] S. Gottlieb-Schönmeyer, S. Brü hne, F. Ritter, W. Assmus, S. Balanetskyy, M. Feuerbacher, T. Weber, and W. Steurer, Crystal growth of copper-rich ytterbium compounds: The predicted giant unit cell structures $YbCu_{4.4}$ and $YbCu_{4.25}$, Intermetallics **17**, 6 (2009).

[8] L. Spendeler, D. Jaceard, J. Sierro, M. François, A. Stepanov, and J. Voiron, Resistivity and thermoelectric power of $YbCu_{4.5}$ under very high pressure, J. Low Temp. Phys. **94**, 585 (1994).

[9] N. Tsujii, J. He, F. Amita, K. Yoshimura, and K. Kosuge, H. Michor, G. Hilscher, and T. Goto, Kondo-lattice formation in cubic-phase $YbCu_5$, Phys. Rev. B **56**, 8103 (1997).

[10] A. Amato, R. A. Fisher, N. E. Phillips, D. Jaccard, and E. Walker, Magnetic field dependence of the specific heat of heavy-fermion $YbCu_{4.5}$, Lawrence Berkeley Laboratory Report, LBL-28747 (1970).

[11] N. Sato, H. Abe, M. Kontani, S. Yamagata, K. Adachi, and T. Komatsubara, Magnetic properties of heavy fermion compounds $YbCu_{3.5}$ and $YbCu_{4.5}$, Physica B (Amsterdam) **163**, 325 (1990).

[12] A. Amato, R. A. Fisher, N. E. Phillips, D. Jaccard, and E. Walker, Pressure dependence of the specific heat of heavy-fermion $YbCu_{4.5}$, Physica B (Amsterdam) **165–166**, 425 (1990).

[13] P. Link, K. Alami-Yadri, D. Jaccard, J. Sierro, and E. Walker, The electrical resistivity of $YbCu_{4.5}$ at high pressure, Physica B (Amsterdam) **206–207**, 361 (1995).

[14] H. Yamaoka, I. Jarrige, N. Tsujii, J.-F. Lin, N. Hiraoka, H. Ishii, and K.-D. Tsuei, Temperature and pressure-induced valence transitions in $YbNi_2Ge_2$ and $YbPd_2Si_2$, Phys. Rev. B **82**, 035111 (2010).

[15] H. Yamaoka, I. Jarrige, N. Tsujii, J.-F. Lin, T. Ikeno, Y. Isikawa, K. Nishimura, R. Higashinaka, H. Sato, N. Hiraoka, H. Ishii, and K.-D. Tsuei, Strong Coupling Between $4f$ Valence Instability and $3d$ Ferromagnetism in $Yb_xFe_4Sb_{12}$ Studied by Resonant X-ray Emission Spectroscopy, Phys. Rev. Lett. **107**, 177203 (2011).

[16] A. P. Hammersley, S. O. Svensson, M. Hanfland, A. N. Fitch, and D. Hausermann, Two-dimensional detector software: From real detector to idealised image or two-theta scan, High Press. Res. **14**, 235 (1996).

[17] H. Yamaoka, Pressure dependence of the electronic structure of $4f$ and $3d$ electron systems studied by x-ray emission spectroscopy, High Press. Res. **36**, 262 (2016).

[18] H. K. Mao and P. M. Bell, High-pressure physics: The 1-Megabar mark on the ruby R_1 static pressure scale, Science **191**, 852 (1976).

[19] K. Syassen, Ruby under pressure, High Press. Res. **28**, 75 (2008).

[20] B. Coqblin and J. R. Schrieffer, Exchange interaction in alloys with cerium impurity, Phys. Rev. **185**, 847 (1969).

[21] V. T. Rajan, Magnetic Susceptibility and Specific Heat of the Coqblin-Schrieffer Model, Phys. Rev. Lett. **51**, 308 (1983).

[22] T. Graf, J. M. Lawrence, M. F. Hundley, J. D. Thompson, A. Lacerda, E. Haanappel, M. S. Torikachvilit, Z. Fisk, and P. C. Canfield, Resistivity, magnetization, and specific heat of $YbAgCu_4$ in high magnetic fields, Phys. Rev. B **51**, 15053 (1995).

[23] N. E. Bickers, D. L. Cox, and J. W. Wilkins, Self-consistent large-N expansion for normal-state properties of dilute magnetic alloys, Phys. Rev. B **36**, 2036 (1987).

[24] P. Link, K. Alami-Yadri, D. Jaccard, J. Sierro, and E. Walker, Unexpected behaviour of $YbCu_{4.5}$ at very high pressures, Z. Phys. B **96**, 145 (1994).

[25] H. Kaga, H. Kubo, and T. Fujiwara, Coherent Kondo lattice state and the crossover transitions in the Anderson-lattice model, Phys. Rev. B **37**, 341 (1988).

[26] R. Černý, M. François, K. Yvon, D. Jaccard, E. Walker, V. Petříček, I. Císařová, H.-U. Nissenk, and R. Wessicken, A single-crystal x-ray and HRTEM study of the heavy-fermion compound $YbCu_{4.5}$, J. Phys.: Condens. Matter **8**, 4485 (1996).

[27] J. He, N. Tsujii, M. Nakanishi, K. Yoshimura, and K. Kosuge, A cubic $AuBe_5$-type $YbCu_5$ phase with trivalent Yb ion, J. Alloy. Compd. **240**, 261 (1996).

[28] V. Petříček, M. Dušek, and L. Palatinus, Crystallographic computing system JANA2006: General features, Z. Kristallogr. **229**, 345 (2014), see also http://jana.fzu.cz/.

[29] H. Yamaoka, I. Jarrige, N. Tsujii, N. Hiraoka, H. Ishii, and K.-D. Tsuei, Temperature dependence of the Yb valence in $YbCu_5$ and $YbCu_{5-x}Al_x$ Kondo compounds studied by x-ray spectroscopy, Phys. Rev. B **80**, 035120 (2009).

[30] H. Yamaoka, N. Tsujii, M.-T. Suzuki, Y. Yamamoto, I. Jarrige, H. Sato, J.-F. Lin, T. Mito, J. Mizuki, H. Sakurai, O. Sakai, N. Hiraoka, H. Ishii, K.-D. Tsuei, M. Giovannini, and E. Bauer, Pressure-induced anomalous valence crossover in cubic $YbCu_5$-based compounds, Sci. Rep. **7**, 5846 (2017).

[31] N. M. Souza-Neto, J. Zhao, E. E. Alp, G. Shen, S. V. Sinogeikin, G. Lapertot, and D. Haskel, Reentrant Valence Transition in EuO at High Pressures: Beyond the Bond-Valence Model, Phys. Rev. Lett. **109**, 026403 (2012).

[32] L. Petit, Z. Szotek, M. Lüders, W. M. Temmerman, and A. Svane, First-principles study of valence and structural transitions in EuO under pressure, Phys. Rev. B **90**, 035110 (2014).

[33] H. Yamaoka, N. Tsujii, K. Yamamoto, A. M. Vlaicu, H. Oohashi, H. Yoshikawa, T. Tochio, Y. Ito, A. Chainani, and S. Shin, Bulk sensitive spectroscopy for the valence transition in $YbInCu_4$-based compounds, Phys. Rev. B **78**, 045127 (2008).

[34] J. M. Lawrence, P. S. Riseborough, C. H. Booth, J. L. Sarrao, J. D. Thompson, and R. Osborn, Slow crossover in $YbXCu_4$ (X = Ag, Cd, In, Mg, Tl, Zn) intermediate-valence compounds, Phys. Rev. B **63**, 054427 (2001).